

Biocompatibility of Nanoscale Hydroxyapatite-embedded Chitosan Films

Fangfang Sun, Kwangnak Koh, Su-Chak Ryu, Dong-Wook Han,* and Jaebeom Lee*

Department of Nanomedical Engineering, College of Nanoscience and Nanotechnology, Pusan National University, Miryang 627-706, Korea. *E-mail: nanohan@pusan.ac.kr (D.-W. H); jaebeom@pusan.ac.kr (J.B. L)

Received June 27, 2012, Accepted September 5, 2012

In order to improve the bioactivity and mechanical properties of hydroxyapatite (HAp), chitosan (Chi) was *in situ* combined into HAp to fabricate a composite scaffold by a sublimation-assisted compression method. A highly porous film with sufficient mechanical strength was prepared and the bioactivity was investigated by examining the apatite formed on the scaffolds incubated in simulated body fluid. In addition, the cytotoxicity of the HAp/Chi composite was studied by evaluating the viability of murine fibroblasts (L-929 cells) exposed to diluted extracts of the composite films. The apatite layer was assessed using scanning electronic microscopy, inductively coupled plasma-optical emission spectrometry and weight measurement. Composite analysis showed that a layer of micro-sized, needle-like crystals was formed on the surface of the composite film. Additionally, the WST-8 assay after L-929 cells were exposed to diluted extracts of the composite indicated that the HAp/Chi scaffold has good *in vitro* cytocompatibility. The results indicated that HAp/Chi composites with porous structure are promising scaffolding materials for bone-patch engineering because their porous morphology can provide an environment conducive to attachment and growth of osteoblasts and osteogenic cells.

Key Words : Hydroxyapatite, Chitosan, Simulated body fluid, Cytotoxicity, Porous structure

Introduction

Bone is a natural ceramic-based organic-inorganic composite,¹ consisting of the collagen and carbonated hydroxyapatite (HAp). In the body, bone served several functions including providing the mechanical properties,² performing a metabolic function³ as well as aiding the body movements.⁴⁻⁶ However, as with any organ, bone diseases including bone loss and defects are encountered clinically with increasing frequency,⁷⁻¹¹ so that the acquisition of novel bone substitutes is becoming extremely urgent in medical research and clinical applications.

So far, several promising scaffold or three-dimensional construction materials have been investigated for tissue engineering due to the necessary support provided for cells to proliferation and their maintained differentiated function. Recently, bioactive ceramic materials (specially HAp), poly(α -hydroxyesters) and natural polymers^{12,13} have attracted much attention from clinicians and medical researchers. Among these compounds, HAp, a well-known bioceramic, is the main inorganic constituent of human hard tissue. With the general formula of $\text{Ca}_{10}(\text{PO}_4)_6(\text{OH})_2$, HAp has extremely close chemical similarity to natural bone, which led to extensive research efforts to use synthetic HAp as a bone substitute and/or replacement in biomedical applications.^{3,14,15}

It was reported that nanocrystalline HAp (nHAp) powders exhibit improved sinterability and enhanced densification due to their enlarged surface area, which may improve fracture toughness.³ Moreover, HAp possesses excellent biocompatibility and considerable mechanical properties as well as the osteoconductivity, and due to the chemical similarity,

HAp facilitates the formation of new bone without resorption and interacts with the living system.¹⁶ Thus HAp can be utilized extensively for the regeneration and reinforcement of damaged bone.^{17,18} However, HAp is limited in the applications of complex forms required for bone treatment due to its intrinsic defects, *e.g.*, brittleness and poor processing properties, HAp powder, used for engineered tissue implants of bone treatment, have the problems of easy shifting from the planted area. On the other hand, natural bone matrix is a typical combination of a naturally occurring polymer (collagen) and a biological mineral (apatite), and blending with inorganic material, which can modify not only the mechanical properties but also the degradation rates of materials. In addition, this natural composite material also has an excellent balance between strength and toughness, superior to either of its individual components. Therefore, it is a natural strategy to combine polymer and HAp to fabricate scaffolds that meet all the requirements desired for particular applications in tissue engineering rather than using a single material type for synthesis.¹⁹

Based on the above reasons, and to utilize the HAp more widely and efficiently in orthopaedic tissue engineering, organic polymers were adopted for compensating the poor mechanical properties of HAp in the treatment of bone regeneration. In addition, HAp-polymer biocomposites scaffold which received increasing attention^{20,21} possess high osteoconductivity,^{22,23} excellent biocompatibility,^{24,25} and moderately biodegradable properties.^{17,26} It was reported that the addition of polymer to the HAp could improve its bioactivity²⁷ and enhance both the mechanical and cell-attachment properties of the scaffolds.^{28,29} In this field, HAp/Chitosan (Chi)

composites have been widely studied for biological applications.²⁹ As we know, Chi is the partially deacetylated form of chitin that is extracted from crustaceans. Additionally, it degrades in the body to non-harmful and non-toxic compounds and has been used in various applications such as nutrition, metal recovery, and biomaterials.³⁰ Based on these advantages, HAp/Chi composites are expected to become a novel scaffolds in biological applications for bone attachment and tissue engineering.

Besides the aforementioned advantage of HAp/Chi composite, for artificial scaffolds, one of the most important descriptions of bioactivity is attributed to the formation of an active bone-like, carbonate containing apatite layer which is chemically and structurally equivalent to the mineral phase in bone and provides an interfacial bonding between materials and tissues.^{1,29,31-33.}

In the previous paper, we fabricated the porous and flexible HAp/Chi film with high mechanical strength by using inherited polymeric phase separation in the solidification process, assisted with compression in film processing, which was called the sublimation-assisted compression (SAC) method.²⁰ While, in this report, the bioactivity and biodegradability of the HAp/Chi scaffold were characterized. In general, the evaluation of HAp composites was performed *via in vitro* tests to observe cell reproduction, proliferation and differentiation, better to investigate the biocompatibility and biodegradability. The cellular viability can be evaluated depending on the cell's proliferative capacity. Osteoblasts usually are used for culturing on a HAp composite scaffold, after proliferation, the viability of the osteoblasts is evaluated by using an MTT assay in the presence of the composites. By comparing the cell performance on a scaffold without HAp, we are able to estimate whether HAp is bioactive as well as characterize whether HAp promotes cell growth and makes the composite scaffold more biodegradable. In this study, the bioactivity of HAp scaffold were characterized by an *in vitro* process using simulated body fluid (SBF) to analyze surface morphology changes with respect to the incubation time of the composite. Additionally, the Ca and P concentrations in the SBF *versus* the immersion time were evaluated *via* inductively coupled plasma/optical emission spectroscopy (ICP-OES) analysis, and the weight loss of composite *versus* the time after immersion in SBF was also investigated. Finally, cell culturing of the composite was processed by using L-929 fibroblastic cells and work-up by WST-8 assay, the situation of the apatite layer formation on different substrates and the impacts on cell's proliferation and difference were discussed, the results indicated that the HAp/Chi scaffold has good *in vitro* bioactivity and cytocompatibility.

Materials and Methods

Materials. Chitosan with deacetylation > 75% and viscosity of 800.00 cps was obtained from Aldrich. Acetic acid with purity of > 97% was purchased from Aldrich (Milwaukee, USA) without further purification.

Preparation of Nanoscale HAp. A 635-mesh ($\leq 20 \mu\text{m}$) HAp powder (Bone Tech[®] Inc., Miryang, Korea), which shows excellent biocompatibility with hard calcified tissues and is similar to the mineral components of bone, was used in this study. Transmission electron microscopy (TEM) and X-ray diffraction (XRD) revealed the HAp powder to have a mean size of 200 nm with a polycrystalline structure. Field emission scanning electron microscopy (FE-SEM) analysis showed that the HAp powder separated using a micro mesh consisted of agglomerates of nanoscale HAp particles, 60 nm in length and 30 nm in diameter, with cylindrical shapes. The majority of the agglomerated powders dispersed in D.I. water with sequential ultra-sonication. ICP-OES analysis confirmed that the weight percentage of CaO and P₂O₅ were 57.0 wt % and 41.4 wt %, respectively. Energy-dispersive X-ray spectroscopy (EDX) showed that the molar ratio of Ca and P was 1.67. The quantitative analysis of the composition from ICP-OES and XRD confirmed that the prepared HAp powder was similar to natural HAp. The detailed experimental results and morphological data can be seen elsewhere.^{12,20}

Preparation of HAp/Chi Composites with Different Ratios. An aqueous 1.0 wt % Chi solution was prepared by dissolving Chi powder in distilled water containing 0.1 M acetic acid. The mixture was stirred at room temperature for 2 h to obtain a homogeneous polymer solution. The amounts of HAp were adjusted to 0 g, 0.125 g, 0.25 g, 0.5 g, 0.75 g, and 1.0 g. The corresponding weight ratios of the HAp/Chi composites were designated as HAp A = 0/5, HAp B = 1/4, HAp C = 1/2, HAp D = 1/1, HAp E = 3/2 and HAp F = 2/1, respectively. The HAp powder was added into the prepared solution with continuous stirring to make a well-dispersed mixture. The mixtures were agitated vigorously in an ultrasonic bath (8510E-DTH, Branson, USA) for approximately 1 h until they showed no precipitation or aggregation.

Preparation of the Composite Films. The prepared mixtures were chilled in a deep freezer (Nihon Freezer, NF-75SF, Japan) at a preset temperature of $-78 \text{ }^\circ\text{C}$ for 4 h, then the frozen mixtures were transferred into a freeze-drying system (FreeZone, Labconco Co., USA) at a preset temperature of $-88 \text{ }^\circ\text{C}$ and a vacuum of 12.0 Pa. The samples were lyophilized for 36 h to remove solvents in the mixture. Finally, the HAp/Chitosan composites were pressed into flexible thin films under a pressure of 10 tons for 10 s with two repetitions by using an auto press (Hyundai Mechanics Inc., Korea). To remove the acetic acid in the mixture, the prepared film was subsequently heated at $120 \text{ }^\circ\text{C}$ for 6 h.

Preparation of SBF Solution. An SBF solution, known to be a metastable buffer solution of human blood plasma, was prepared by dissolving appropriate quantities of the reagent-grade chemicals NaCl, NaHCO₃, KCl, K₂HPO₄·3H₂O, MgCl₂·6H₂O, Na₂SO₄, and CaCl₂·2H₂O in deionized water. Tris(hydroxymethyl)aminomethane was used to buffer the SBF solution, and the pH value was adjusted to 7.25 at 36.5 $^\circ\text{C}$ by adding 1 M HCl before the addition of CaCl₂ to prevent the formation of a precipitate. The ion concentrations of the prepared SBF are shown in Table 1.

Table 1. Ion concentrations of prepared simulated body fluid and human blood plasma

Ion	Concentration (mmol/dm ³)	
	Simulated body fluid (SBF)	Human blood plasma
Na ⁺	142.0	142.0
K ⁺	5.0	5.0
Mg ²⁺	1.5	1.5
Ca ²⁺	2.5	2.5
Cl ⁻	147.8	103.0
HCO ₃ ⁻	4.2	27.0
HPO ₄ ²⁻	1.0	1.0
SO ₄ ²⁻	0.5	0.5

Characterization of the HAp/Chi Nanocomposite Scaffold. The physicochemical and morphological property assessments of the composite films after immersion in SBF were carried out by FE-SEM (Hitachi S4700, Osaka, Japan).²⁰ Mechanical properties were measured by a materials testing machine (LLOYD, AMETEK, England) at a crosshead speed of 5 mm/min and a span of 10 mm. Five 15 × 10 mm rectangular pieces were measured 5 times, and the results were averaged. The bioactivities were characterized by ICP-OES. Moreover, the variations in the concentrations of Ca and P of the composite after immersion in SBF *versus* soaking time were also measured. The cytotoxicity of the composite films was assessed by evaluating the viability of L-929 fibroblastic cells exposed to their diluted extracts.

In vitro Degradation/Bioactivity Tests in SBF. SBF has been widely used as a rapid and effective method to investigate the bioactivity and biocompatibility of composite scaffolds. Typically, we evaluated the bioactivity of the HAp/Chi nanocomposite scaffold *in vitro* by immersing a representative specimen (HAp D, weight ratio = 1/1) in SBF. The specimen (0.0216 g) was placed into SBF (50 mL) in an incubator at 37.8 °C. The concentrations of Ca and P ions in the SBF were determined with ICP-OES at 20 h intervals and then at three months after immersion without daily change of the SBF. For weight measurement and FE-SEM observations of morphological changes, after the pre-selected soaking time the specimen was gently rinsed with distilled water to remove the surface SBF solution and dried naturally in a desiccator.

Cytotoxicity Assay. A murine fibroblast cell line (L-929 cells, from subcutaneous connective tissue) was obtained from the American Type Culture Collection (CCL-1™, Rockville, MD). The cells were routinely maintained in Dulbecco's modified Eagle's medium (Sigma-Aldrich Co., St. Louis, MO) supplemented with 10% fetal bovine serum (Sigma-Aldrich Co.) and 1% antibiotic antimycotic solution (including 10,000 U penicillin, 10 mg streptomycin, and 25 mg amphotericin B per mL, Sigma-Aldrich Co.) at 37 °C in a humidified atmosphere of 5% CO₂ in air. The number of viable cells was indirectly quantified using a highly water-soluble tetrazolium salt [WST-8, 2-(2-methoxy-4-nitrophenyl)-3-(4-nitrophenyl)-5-(2,4-disulphophenyl)-2H-tetrazolium,

mono-sodium salt] (Dojindo Lab., Kumamoto, Japan), reduced to formazan dye by mitochondrial dehydrogenases. The cell viability (cytotoxicity) was found to be directly proportional to the metabolic reaction products obtained in WST-8. Briefly, the WST-8 assay was conducted as follows. L-929 cells were treated with diluted extracts of HAp/Chi composites A-F and then incubated with WST-8 for the last 4 h of the culture period (24 h) at 37 °C in the dark. Parallel sets of wells containing freshly cultured cells were regarded as negative (-) controls. As positive (+) controls, 1.25%-20% dimethyl sulfoxide (DMSO) was employed. The absorbance was determined at 450 nm using an enzyme-linked immunosorbent assay (ELISA) reader (SpectraMax® 340, Molecular Device Co., Sunnyvale, CA). The relative cell viability was determined as the percentage ratio of the optical densities in the medium containing serially diluted concentrations (6.25%-100%) of HAp/Chi films to that in the fresh control medium. The IC₅₀ of DMSO [the concentration (%) inhibiting the growth of cells by 50%] was estimated from the relative cell viability profile. At the end of the incubation, the cellular morphology was observed using an inverted microscope (IX70, Olympus Optical, Osaka, Japan).

Results and Discussion

Physicochemical Characterizations of HAp/Chi Composites. The morphology of the film was characterized by SEM as shown in Figure 1. Both Chi and the other HAp composites exhibited a highly homogeneous and porous structure: the porosity of the film was evaluated with a liquid displacement method using ethanol as the displacing liquid following Zhang's method.¹³ The porosity of the HAp D scaffold was calculated as (89.45 ± 0.68)%, and the porosity of Chitosan scaffold is (89.16 ± 0.37)%. Based on our previous report,²⁰ the composite HAp D with uniform porous structure possessed the optimal combination of Chi and HAp due to the optimized properties it exhibited. Therefore, the HAp D composite (weight ratio = 1/1) was selected as a

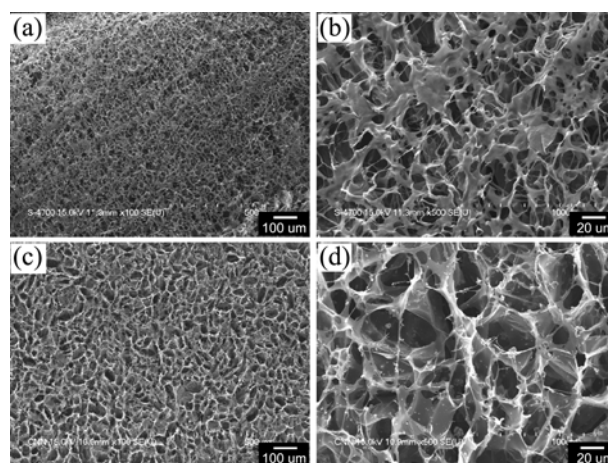


Figure 1. SEM images of the porous structure of (a and b) the Chi scaffold and (c and d) the composite HAp D (weight ratio = 1/1); (b) and (d) are the magnifications of (a) and (c), respectively.

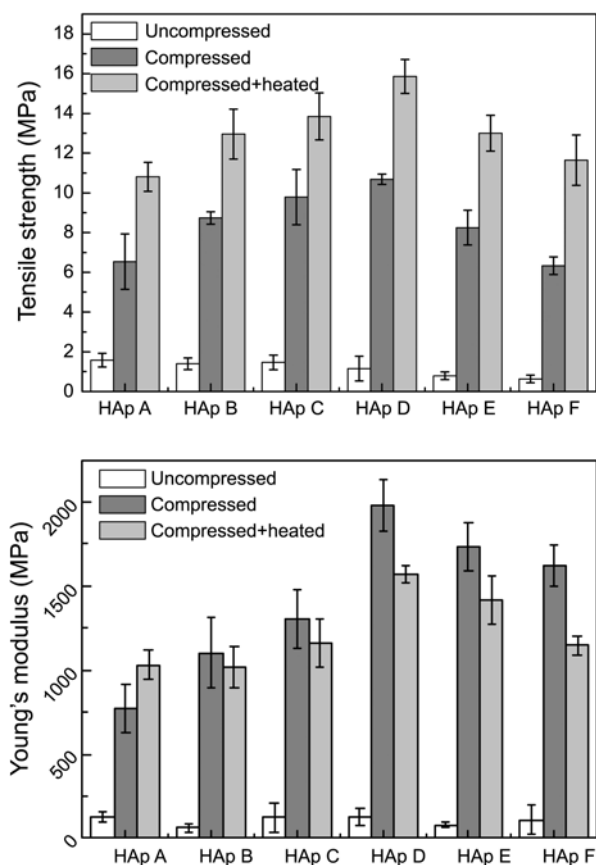


Figure 2. Mechanical properties (including the tensile strength and young's modulus) of HAp/Chi scaffold with various weight ratio.

representative specimen for further analysis and comparison with the Chi (HAp A) scaffold in the following bioactivity assessments and characterizations.

The mechanical properties of the HAp-chitosan films based on the composition ratio (w/w %) were investigated in Figure 2. Average tensile strength and Young's modulus of the as-fabricated HAp/chitosan composite were approximately 1.17 ± 0.38 MPa and 104 ± 27.8 MPa, respectively. Interestingly, these values are significantly higher than values reported elsewhere.³⁴ This may due to the different experimental conditions, such as compression, pore size, water moisture ratios and alignment of the film structure. Mechanical properties of HAp/Chi composite, including the tensile strength and Young's modulus, significantly increased up to 20 times after compression. In addition, it was clearly seen that both of the tensile strength and Young's modulus increased dramatically with increasing HAp content (until HAp/chitosan ratio of 100 w/w %). Addition of HAp powder may also be the major reason for increased strength in the films,³⁵ during the high compression, enhanced chemical bonding can develop in the proximity of the chitosan layers, which would induce a higher mechanical strength. On the other hand, exceeding a critical amount of HAp particles in the chitosan matrix could result in phase separation and less chemical bonding between HAp and chitosan. Therefore, in view of the surface morphology, as well as the mechanical

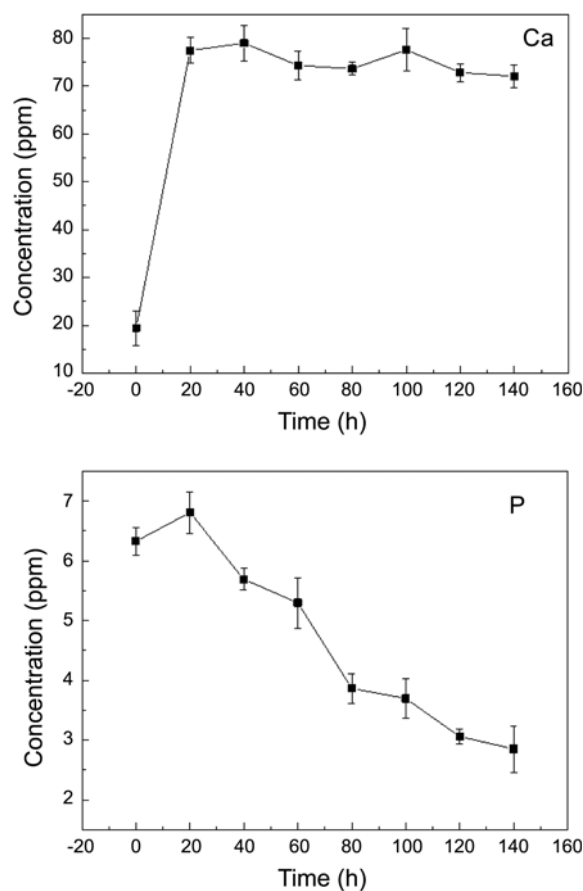


Figure 3. Ca and P concentrations versus soaking time after immersion of the composite HAp D (weight ratio = 1/1) in SBF.

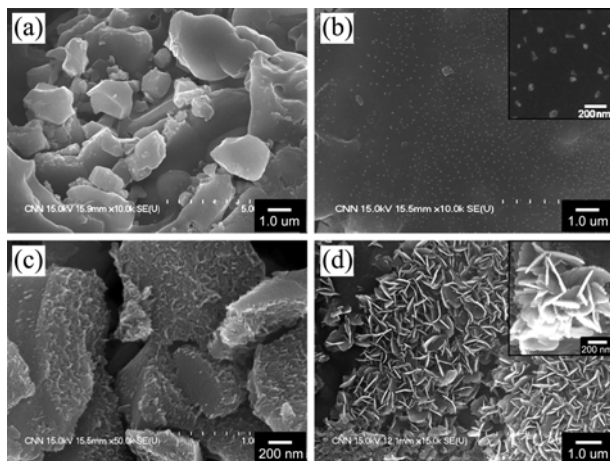
properties, HAp-chitosan ratio of 100 w/w % (HAp D) would be the optimum composite. That is the reason why we selected HAp D as a representative specimen in this study for comparing with Chi (HAp A) scaffold.

The biodegradability investigation of the HAp/Chi composite (HAp D) was carried out to observe the surface morphology and composition changes by means of SEM-EDX analysis and ICP-OES characterization, as well as to observe cell cytotoxicity *via in vitro* testing. The variations of Ca and P concentrations in SBF as a function of soaking time are shown in Figure 3. Initially, rapid Ca release from the specimen to the solution is observed for the HAp D film as long as it was soaked in SBF, after which the calcium concentration increases marginally in the following 20 h. Finally, it gets to a plateau and maintained until the end of the experiment (after 140 h soaking in SBF). These results indicate that Ca ion is released from the specimen to the fluid, which is consistent with the initial weight loss of the specimen as described in Table 2. In contrast, the phosphorus concentration of the SBF initially does not vary and it decreased slightly over the following 20 h. Furthermore, the specimen showed no signs of releasing after incubated for 140 h.

The morphologies of the biomimetic coatings formed on the surfaces of the HAp/Chi films were investigated by FE-SEM (Figure 4). A slight dissolution on the surface and

Table 2. The weight distribution of the composite HAp D (weight ratio = 1/1, original weight: 0.0216 g) after soaking in SBF

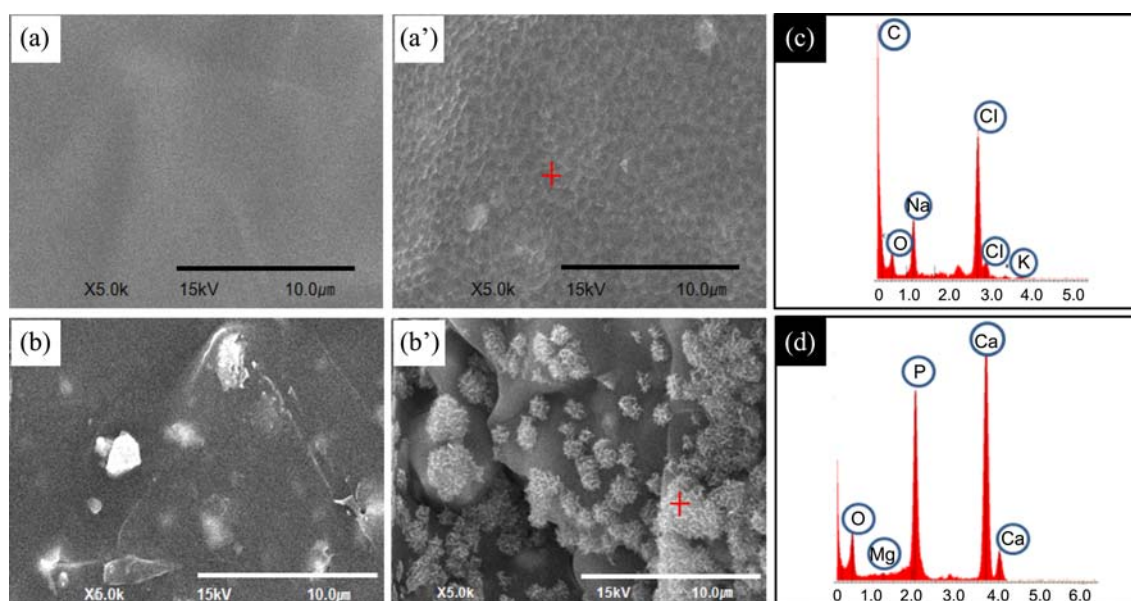
Time (day)	1	2	3	4	5	6	7
Weight (g)	0.0192	0.0194	0.0198	0.0193	0.0202	0.0206	0.0209

**Figure 4.** SEM images of the composite HAp D after immersion in SBF solution for (a) 60 h, (b) 120 h, (c) 140 h and (d) 3 months. Inserts of B and D indicate their respective magnified images.

edges of the film was observed, which indicated that the solution concentration of Ca and P ions increased initially after immersion in SBF, moreover, it was observed that nano-sized HAp was homogeneously dispersed in the polymer phase of Chi. Further, HAp/Chi composite with rough surface morphology was examined. As soaking time increased, many needle-like particles formed on the surface of the composite (Figure 4(b)), and subsequently grew to micro-sized crystals with needle-like structure (Figure 4(c)). Finally, larger clusters with petaloid shapes resulted after soaking in SBF for three months. Figure 4(d) depicts the surface morphology of the

HAp D (weight ratio = 1/1) scaffold after soaking in SBF for three months. Significantly, a new coating layer of crystalline aggregates with needle-like structure covered the surface of the specimen. In addition, uniform and increased larger area of crystalline clusters was observed compared with the scaffold after soaking in SBF for 1 week. In summary, these assessments indicate that long SBF-soaking times produced larger areas coated with needle-like crystalline aggregates on the surface.

As showed in Figure 5, the SEM-EDX analysis of the crystalline aggregate confirmed the presence of calcium and phosphorus in the layer deposited on the surface of the HAp/Chi composite scaffold after soaking in SBF. Moreover, EDX detection showed the principal elements of the crystalline deposition were Ca and P. The examined Ca/P ratio of the aggregate ranges from 1.6 to 1.74 and the mean Ca/P ratio of the deposition is 1.65, which was strongly suggestive of bone-like HAp, for which the theoretical value of pure HAp is 1.67.³⁶ Many researches based on the biomimetic properties of composites have been published, for instance, Lickorish and coworkers³⁷ reported the EDX spectrum of a collagen/HAp composite after treatment in SBF, and found that several fields gave a semi-quantitative Ca/P ratio of 1.61 ± 0.23 . In addition, Yang *et al.*³⁸ investigated the biomimetic process for electrospun poly(ϵ -caprolactone) scaffolds, and EDX results showed that the Ca/P ratio of the coating was around 1-1.2. Compared with the results of Lickorish and Yang, the HAp/Chi composite in our study exhibited much higher biomimetic properties. In general, the process that

**Figure 5.** SEM images of the Chi film before (a) and after (a') immersion in SBF for 1 week and the HAp D film before (b) and after (b') immersion in SBF for 11 days. (c) and (d) are the results from EDX analysis showing the points in the films (a') and (b'), respectively.

presumably occurred involves both deposition and crystallization of SBF-derived Ca, P, and O ions on the surface of the scaffold to form the bone-like HAp crystals. In addition, we found that the crystallization of these ions is in proportion to the length of immersion time, and the length of time in which samples were dipped in SBF significantly affected the extent of coating as well as the crystalline arrangement. The time-dependent nature of this crystalline aggregation is in agreement with the assessment characterized by ICP-OES. In contrast, there was no deposition of a Ca-P phase or apatite observed on the surface of the Chi film. Instead, a Na-Cl phase in form of NaCl was identified as shown in Figure 5(a'). Compared with the HAp/Chi composite (Figure 5(b)), the results indicated significantly that only in the case in which the scaffold contained HAp was possible to form the HAp nuclei and deposit crystalline apatite.

Cytotoxicity of HAp/Chi Composites. Cytotoxicity profiles of HAp/Chi composites A-F were determined in L-929 fibroblastic cells by the WST-8 assay. The cells exposed to increasing concentrations (6.25%-100%) of diluted extracts of each composite for 24 h showed no dose-dependent decrease in their relative cell viability (Figure 6(a)). Among those composites, HAp/Chi composites A, B and C showed slight fluctuations in the relative cell viability, which was not

significantly different from that of the non-treated control. In the cells treated with increasing concentrations (1.25%-20%) of DMSO, however, the cell viability was remarkably decreased in a dose-dependent manner. The IC_{50} value (%) of DMSO against L-929 cells was found to be about 4.72%. In contrast, the IC_{50} values of all films could not be determined from the cytotoxicity profiles. Cellular responses to 10% DMSO and 50% diluted extracts of each composite were evident from morphological observations (Figure 6(b)). The cells treated with 50% concentrations of the diluted extracts of all composites exhibited typical fibroblast-like phenotypes, with a few alterations in the cellular morphologies, which were almost the same with those of the non-treated control. When exposed to 10% DMSO, however, most of the cells showed characteristic morphologies of cells undergoing apoptosis including blebbing and changes to the cell membrane such as loss of membrane asymmetry and attachment, and even cell shrinkage.³⁹ This result implies that HAp/Chi composites are cytocompatible *in vitro* irrespective of the composition ratio of HAp/Chi.

Conclusion

HAp/Chi nanocomposites were prepared by freeze-drying associated with the solvent evaporation method described in our previous paper.²⁰ In the current study, the obtained nanocomposite scaffold was characterized by soaking in SBF to investigate the bioactivity and biocompatibility; it was found that the HAp/Chi composite scaffold exhibited a needle-like structural growth after 140 h SBF incubation; likewise, a considerable amount of surface coating with petaloid-shapes clusters of bone-like HAp after incubation for three month also was investigated. Additionally, cell culturing of the composite with L-929 fibroblastic cells and work-up by WST-8 assay indicated that the HAp/Chi scaffold has good *in vitro* bioactivity and cytocompatibility. Based on the above *in vitro* test of bioactivity and biodegradability characterization associated with HAp/Chi composite, it is reasonable to deduce that the prepared HAp/Chi composite has the potential to be applied in bio-applications, such as bone patching and bone-substitute materials.

Acknowledgments. This research was supported partly by the Korea Health Care Technology R&D Project, Ministry of Health & Welfare, Republic of Korea (A A110191-1101-0000200), the International Research & Development Program of the National Research Foundation of Korea (NRF) funded by the Ministry of Education, Science and Technology (MEST) of Korea (Grant number: K20903002036-11B1200-15110) and the New & Renewable Energy program of the Korea Institute of Energy Technology Evaluation and Planning (KETEP) grant (No. 20103020010050) funded by the Ministry of Knowledge Economy, Republic of Korea.

References

1. Rezwan, K.; Chen, Q. Z.; Blaker, J. J.; Boccaccini, A. R. *Biomaterials*

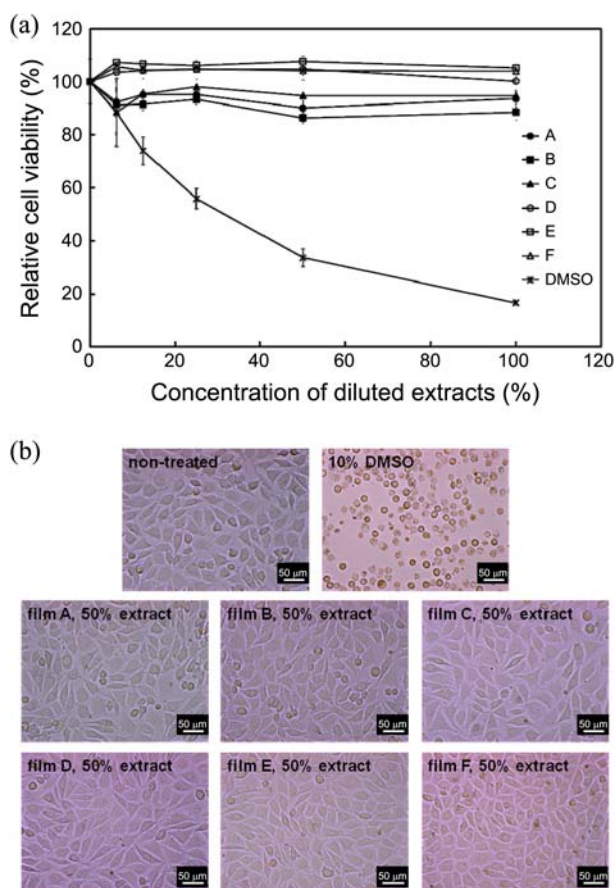


Figure 6. (a) Relative cell viability profile and (b) optical micrographs of cell morphologies of L-929 cells 24 h after treatment with diluted extracts of HAp/Chi composites A-F. In (a), 20% DMSO was the maximum concentration, considered as 100%.

- 2006, 27, 3413.
- Weiner, S.; Wagner, H. D. *Annu. Rev. Mater. Sci.* **1998**, 28, 271.
 - Zhou, H.; Lee, J. *Acta Biomaterialia* **2011**, 7, 2769.
 - Poinern, G. E.; Brundavanam, R. K.; Mondinos, N.; Jiang, Z. T. *Ultrason. Sonochem.* **2009**, 16, 469.
 - Hellmich, C.; Ulm, F. J. *Biomech. Model. Mechanobiol.* **2003**, 2, 21.
 - Dorozhkin, S. V. *Acta Biomaterialia* **2010**, 6, 715.
 - Zhao, H.; Ma, L.; Gao, C.; Shen, J. *Polym. Adv. Technol.* **2008**, 19, 1590.
 - Brown, G. D.; Mealey, B. L.; Nummikoski, P. V.; Bifano, S. L.; Waldrop, T. C. *J. Periodontol.* **1998**, 69, 146.
 - Kimelman, N.; Pelled, G.; Helm, G. A.; Huard, J.; Schwarz, E. M.; Gazit, D. *Tissue Eng.* **2007**, 13, 1135.
 - Bruder, S. P.; Jaiswal, N.; Ricalton, N. S.; Mosca, J. D.; Kraus, K. H.; Kadiyala, S. *Clin. Orthop. Relat. Res.* **1998**, 355.
 - Vescovi, J.; Jamal, S.; De Souza, M. *Osteoporosis Int.* **2008**, 19, 465.
 - Ryu, S. C.; Lim, B. K.; Sun, F.; Koh, K.; Han, D. W.; Lee, J. *Bull. Korean Chem. Soc.* **2009**, 30, 887.
 - Zhang, Y.; Zhang, M. *J. Biomed. Mater. Res.* **2001**, 55, 304.
 - Habraken, W.; Wolke, J. G. C.; Jansen, J. A. *Adv. Drug Deliv. Rev.* **2007**, 59, 234.
 - Hutmacher, D. W.; Schantz, J. T.; Lam, C. X. F.; Tan, K. C.; Lim, T. C. *J. Tissue Eng. Regen. Med.* **2007**, 1, 245.
 - Pielichowska, K.; Blazewicz, S. *Advances in Polymer Science*; Springer: 2010; Vol. 232, p 97.
 - Kim, S. H.; Lim, B. K.; Sun, F.; Koh, K.; Ryu, S. C.; Kim, H. S.; Lee, J. *Polymer Bulletin* **2009**, 62, 111.
 - Zou, Q.; Li, Y.; Zhang, L.; Zuo, Y.; Li, J.; Li, X. *J. Biomed. Mater. Res. B: Appl. Biomater.* **2009**, 90B, 156.
 - Sun, F.; Zhou, H.; Lee, J. *Acta Biomaterialia* **2011**, 7, 3813.
 - Sun, F.; Lim, B. K.; Ryu, S. C.; Lee, D.; Lee, J. *Mater. Sci. Eng. C* **2010**, 30, 789.
 - Sun, F.; Cha, H. R.; Bae, K. E.; Hong, S.; Kim, J. M.; Kim, S. H.; Lee, J.; Lee, D. *Mater. Sci. Eng. A* **2011**, 528, 6636.
 - Chang, B. S. *Biomaterials* **2000**, 21, 1291.
 - Woodard, J. R.; Hilldore, A. J.; Lan, S. K.; Park, C. J.; Morgan, A. W.; Eurell, J. A. C.; Clark, S. G.; Wheeler, M. B.; Jamison, R. D.; Wagoner Johnson, A. J. *Biomaterials* **2007**, 28, 45.
 - Itoh, S.; Kikuchi, M.; Takakuda, K.; Koyama, Y.; Matsumoto, H. N.; Ichinose, S.; Tanaka, J.; Kawachi, T.; Shinomiya, K. *J. Biomed. Mater. Res.* **2001**, 54, 445.
 - Liu, C.; Wang, W.; Shen, W.; Chen, T.; Hu, L.; Chen, Z. *J. Endodont.* **1997**, 23, 490.
 - Ito, M.; Hidaka, Y.; Nakajima, M.; Yagasaki, H.; Kafrawy, A. H. *J. Biomed. Mater. Res.* **1999**, 45, 204.
 - Rizzi, S. C.; Heath, D. J.; Coombes, A. G. A.; Bock, N.; Textor, M.; Downes, S. J. *Biomed. Mater. Res.* **2001**, 55, 475.
 - Lin, H. R.; Yeh, Y. J. *J. Biomed. Mater. Res. B: Appl. Biomater.* **2004**, 71B, 52.
 - Kong, L.; Gao, Y.; Lu, G.; Gong, Y.; Zhao, N.; Zhang, X. *Eur. Polym. J.* **2006**, 42, 3171.
 - Im, K. H.; Park, J. H.; Kim, K. N.; Kim, K. M.; Choi, S. H.; Kim, C. K.; Lee, Y. K. *Key Eng. Mat.* **2005**, 284, 729.
 - Song, W. H.; Jun, Y. K.; Han, Y.; Hong, S. H. *Biomaterials* **2004**, 25, 3341.
 - Kokubo, T.; Takadama, H. *Biomaterials* **2006**, 27, 2907.
 - Kokubo, T.; Kim, H. M.; Kawashita, M. *Biomaterials* **2003**, 24, 2161.
 - Madhally, S. V.; Matthew, H. W. T. *Biomaterials* **1999**, 20, 1133.
 - Xianmiao, C.; Yubao, L.; Yi, Z.; Li, Z.; Jidong, L.; Huanan, W. *Mater. Sci. Eng. C* **2009**, 29, 29.
 - Wang, H.; Lee, J. K.; Moursi, A.; Lannutti, J. J. *J. Biomed. Mater. Res. A* **2003**, 67A, 599.
 - Lickorish, D.; Ramshaw, J. A. M.; Werkmeister, J. A.; Glattauer, V.; Howlett, C. R. *J. Biomed. Mater. Res. A* **2004**, 68A, 19.
 - Yang, F.; Wolke, J. G. C.; Jansen, J. A. *Chem. Eng. J.* **2008**, 137, 154.
 - Hacker, G. *Cell Tissue Res.* **2000**, 301, 5.
-